Carrier Frequency Offset Estimation for OFDM Systems using Repetitive Patterns

Yinsheng LIU, Zhenhui TAN

Institute of Broadband Wireless Mobile Communications and State Key Laboratory of Rail Traffic Control and Safety, Beijing Jiaotong University, Beijing 10044, China

09111035@bjtu.edu.cn, zhhtan@bjtu.edu.cn

Abstract. *This paper deals with Carrier Frequency Offset (CFO) estimation for OFDM systems using repetitive patterns in the training symbol. A theoretical comparison based on Cramer Rao Bounds (CRB) for two kinds of CFO estimation methods has been presented in this paper. Through the comparison, it is shown that the performance of CFO estimation can be improved by exploiting the repetition property and the exact training symbol rather than exploiting the repetition property only. The selection of Q (number of repetition patterns) is discussed for both situations as well. Moreover, for exploiting the repetition and the exact training symbol, a new numerical procedure for the Maximum-Likelihood (ML) estimation is designed in this paper to save computational complexity. Analysis and numerical result are also given, demonstrating the conclusions in this paper.*

Keywords

OFDM, CFO, repetitive patterns.

1. Introduction

The OFDM transmission has been widely used in modern communication systems, due to its robustness against the frequency selectivity in wireless channel [1]. The utilization of Cyclic Prefix (CP) enables OFDM system to convert a frequency selective channel into a parallel collection of frequency flat channels, leading to greatly simplified equalizer design [2]. OFDM has been of interest for wireless broadcasting, Wireless MAN [3][4].

Some of the existing CFO estimation algorithms performs CFO estimation by only exploiting the repetitive patterns in the training symbol [5]-[9]. When a training symbol with repetition property is transmitted, the receiver can acquire the CFO estimation based on the auto-correlation of the received signal without exact knowledge on the training symbol. A simple case is that the training symbol is repeated only twice [5]. There are also methods where the training symbol is repeated more than twice [6][7]. By taking the

correlation between any two patterns (adjacent or not) for the CFO estimation, better accuracy can be obtained in [8]. The proposed method in [8] is actually ML-based in the case of more than two repetition patterns under the condition of AWGN channel. On the other side, there are also literatures, focusing on CFO estimation by exploiting both repetitions and exact training symbol [10][11]. In [10], the CRB bound for CFO estimation is derived for frequency selective channel. Based on the derived CRB representation, the optimal design of subblock is investigated in [10]. By exploiting both the repetition property and the exact training symbol, a ML-based estimation of CFO is proposed in [11]. To solve the corresponding likelihood equation, a two-step searching procedure is employed, which may consume great computation complex.

Although excellent works have been done by adopting both strategies, a comparison is never provided in the existing literature. In this paper, that comparison is given by exploiting the CRB representations in both situations. This theoretical comparison clearly shows that we can obtain improved performance by exploiting not only the repetitions but also the exact training symbol. With this theoretical conclusion, newly designed algorithm should focus on exploiting both repetitions and exact training symbol since it can provide a better performance. For exploiting the repetitions and exact training symbol, a new numerical procedure is described in this paper to solve the ML-estimation, which can greatly save the computational complexity.

The rest of this paper is organized as follows. The signal model is given in Section 2. The CRB bounds for both two cases in Additive White Gaussian Noise (AWGN) channel are derived and compared in Section 3. Section 4 derives the proposed algorithm in a ML manner. Performance analysis and numerical results are provided in Section 5 and Section 6, finally the conclusion is dropped in Section 7.

2. Signal Model

Consider an OFDM transmission from transmitter to receiver where a known training symbol is transmitted at the beginning of each frame. The known training symbol can be

represented as

$$s[k] = \frac{1}{\sqrt{N}} \sum_{n=0}^{N-1} X[n] \exp\left(-j\frac{2\pi kn}{N}\right) \qquad (1)$$

where $k \in [-N_{CP}, N-1]$ and N, N_{CP} are the subcarrier number and length of Cyclic Prefix (CP) respectively. $X(n)$ are the frequency domain symbols mapped on each subcarrier. Due to repetition pattern of the training symbol, adjacent non zero frequency domain symbols are equally spaced by $Q-1$ subcarriers. Let M denote the length of each repetition block, so that $M = N/Q$. Owing to frequency selectivity of wireless channel and CFO, the received signal is given by

$$r[k] = (s[k] * h[k]) \exp\left(j\frac{2\pi k\varepsilon}{N}\right) + w[k] \qquad (2)$$

where $*$ denotes the linear convolution. $h[k]$ and $w[k]$ are the channel response (length L) and additive noise, respectively. ε is the CFO normalized by one subcarrier spacing. Since this paper only concern CFO estimation, the timing synchronization is assumed to be perfect. Under this assumption, the CP in the received signal can be easily removed, then the received signal can be represented in matrix form as

$$\mathbf{r} = \mathbf{FSh} + \mathbf{w}. \qquad (3)$$

Here, $\mathbf{r} = (r[0], r[1], \cdots, r[N-1])^T$. $\mathbf{F}$ is a diagonal matrix $\mathbf{F} = \mathrm{diag}\left\{1, \exp\left(j\frac{2\pi\varepsilon}{N}\right), \cdots, \exp\left[j\frac{2\pi\varepsilon(N-1)}{N}\right]\right\}$. $\mathbf{h}$ is a channel response vector with length L, i.e. $\mathbf{h} = (h[0], \cdots, h[L-1])^T$. $\mathbf{w}$ denotes the additive noise vector with covariance matrix $\sigma_w^2 \mathbf{I}$. $\mathbf{A}^T$ denotes the transpose of matrix or vector $\mathbf{A}$. It can be observed that, due to repetition patterns, the matrix $\mathbf{S}$ may be written as

$$\mathbf{S} = [\mathbf{S}_0^T, \mathbf{S}_0^T, \cdots, \mathbf{S}_0^T]^T \qquad (4)$$

where $\mathbf{S}_0$ is an $M \times L$ matrix with elements

$$[\mathbf{S}_0]_{(m,n)} = s[(m-n)_M]. \qquad (5)$$

Here, $0 \leq m \leq M-1, 0 \leq n \leq L-1$ and $(m-n)_M$ means m-n modulo M.

Note that in AWGN channel, with a unknown initial phase θ, the received signal may be written as

$$\mathbf{r} = \mathbf{Fs} \exp(j\theta) + \mathbf{w}. \qquad (6)$$

It is observed that we cannot obtain (6) by simply making $\mathbf{h} = 1$ in (3). Actually, the unknown initial phase θ should always exits due to unsynchronized carriers in the transmitter and the receiver. However, the initial phase may be combined with channel response in frequency selective channel, leading to implicit unknown initial phase in (3). While in AWGN channel, the unknown initial phase is explicitly represented with θ in (6). Accordingly, matrix $\mathbf{S}$ is reduced to vector $\mathbf{s}$ in AWGN channel, where $\mathbf{s}$ can be written as $\mathbf{s} = (\mathbf{s}_0^T, \mathbf{s}_0^T, \cdots, \mathbf{s}_0^T)^T$ and $\mathbf{s}_0 = (s[0], s[1], \cdots, s[M-1])^T$.

3. Cramer Rao Bounds: Comparison

In this section, we present a comparison between the situation where only repetition property is exploited and the situation where both repetitions and the exact training symbol is in use. For simplicity, we only focus on the CRBs in AWGN channel.

3.1 Case I: Repetition Property Only

Suppose a transmitted signal is received in AWGN channel, as represented in (6). Since the transmitted signal is independent of noise, the received signal can be modeled as a Gaussian random process with the following correlation properties

$$E\{r^*[k]r[k+m]\} = \begin{cases} \sigma_s^2 + \sigma_w^2 & m = 0, \\ \sigma_s^2 \exp\left(j\frac{2\pi q\varepsilon}{Q}\right) & m = qM, \\ 0 & \text{otherwise} \end{cases} \qquad (7)$$

where $q = 1, 2, \cdots, Q-1$. Note that (7) holds only for $k \in [0, 1, \cdots, M-1]$. It can be observed from (7) that the probability distribution function (PDF) has no relation with initial phase θ.

If we define $\mathbf{y}_k = (r[k], r[k+M], \cdots, r[k+(Q-1)M])^T$ for $k \in [0, 1, \cdots, M-1]$, then the PDF of vector $\mathbf{r}$ can be represented as

$$f(\mathbf{r}; \varepsilon) = \prod_{k=0}^{M-1} f(\mathbf{y}_k; \varepsilon) \qquad (8)$$

where, $f(\mathbf{y}_k; \varepsilon)$ is given by

$$f(\mathbf{y}_k; \varepsilon) = \frac{1}{\pi^Q \det \mathbf{K}} \exp\left(-\mathbf{y}_k^H \mathbf{K}^{-1} \mathbf{y}_k\right) \qquad (9)$$

where $\mathbf{A}^H$ denotes the conjugate transpose of matrix or vector $\mathbf{A}$. In (9), $\mathbf{K}$ is a $Q \times Q$ correlation matrix whose (m, n)th element is $E\{r[k+mM]r^*[k+nM]\}$, where $k \in [0, 1, \cdots, M-1]$ and $m, n \in [0, 1, \cdots, Q-1]$.

Then, following the derivation in [9], the derived CRB of ε in Case I is found to be

$$\mathrm{CRB1} = \frac{3Q^2}{2\pi^2 N(Q^2-1)}\left(\mathrm{SNR}^{-1} + \frac{\mathrm{SNR}^{-2}}{Q}\right) \qquad (10)$$

where SNR is defined as $\mathrm{SNR} = \sigma_s^2 / \sigma_w^2$. In high SNR condition, the term SNR^{-2} may be omitted and the derived CRB1 in (10) is then reduced to

$$\mathrm{CRB1} = \frac{3\mathrm{SNR}^{-1}}{2\pi^2 N(1-Q^{-2})} \qquad (11)$$

which is as same as the one derived in [6].

3.2 Case II: Both Repetition Property and Exact Training Symbol

In Case II, we focus on deriving the CRB when both repetition property and exact training symbol are exploited. Define $\mathbf{r}_q = (r[(q-1)M], r[(q-1)M+1], \cdots, r[(q-1)M+M-1])^T$ for $q = 1, 2, \cdots, Q$, then the PDF of $\mathbf{r}$ can be represented by
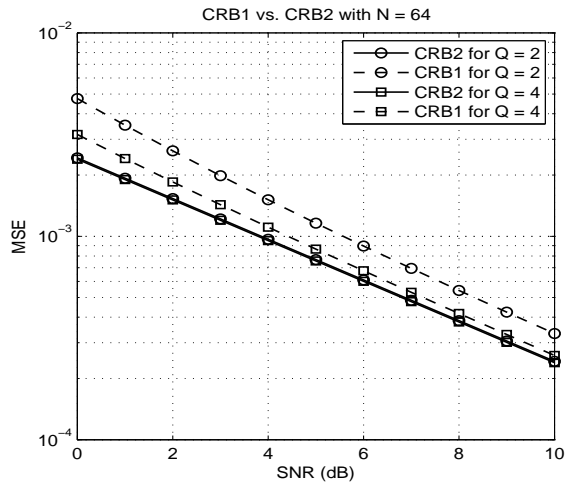
Fig. 1. Comparison between CRB1 and CRB2.

$$f(\mathbf{r};\theta,\varepsilon) = \prod_{q=1}^{Q} f(\mathbf{r}_q;\theta,\varepsilon). \tag{12}$$

Since the training symbol is also utilized, the vector $\mathbf{s}$, as well as $\mathbf{s}_0$, are both known to the receiver. Noting the following relation,

$$\mathbf{r}_q = \mathbf{F}_0\mathbf{s}_0 e^{j[\theta+2\pi\varepsilon(q-1)/Q]} + \mathbf{w}_q, \tag{13}$$

the PDF of $\mathbf{r}_q$ can be obtained as

$$f(\mathbf{r}_q;\theta,\varepsilon) = \tag{14}$$
$$\frac{1}{(\pi\sigma_w^2)^M} \exp\left(-\frac{1}{\sigma_w^2} \left\| \mathbf{r}_q - \mathbf{F}_0\mathbf{s}_0 e^{j[\theta+2\pi\varepsilon(q-1)/Q]} \right\|^2\right)$$

where $\mathbf{F}_0$ is given by

$$\mathbf{F}_0 = \mathrm{diag}\left\{1, \exp\left(j\frac{2\pi\varepsilon}{N}\right), \cdots, \exp\left[j\frac{2\pi\varepsilon(M-1)}{N}\right]\right\}.$$

Since the PDF in (12) depends on two parameters (i.e. θ and ε), Fisher information matrix has to be employed to derive the CRB of ε. Following the definition in [12], the Fisher information matrix in Case II can be written as

$$\mathbf{U} = \begin{pmatrix} E\left[\frac{\partial^2 \ln f(\mathbf{r};\theta,\varepsilon)}{\partial\theta^2}\right] & E\left[\frac{\partial^2 \ln f(\mathbf{r};\theta,\varepsilon)}{\partial\theta\partial\varepsilon}\right] \\ E\left[\frac{\partial^2 \ln f(\mathbf{r};\theta,\varepsilon)}{\partial\theta\partial\varepsilon}\right] & E\left[\frac{\partial^2 \ln f(\mathbf{r};\theta,\varepsilon)}{\partial\varepsilon^2}\right] \end{pmatrix}. \tag{15}$$

Let $\mathbf{U}^{-1}$ be the inverse of $\mathbf{U}$, then the CRB for the estimation of ε is expressed as

$$\mathrm{CRB2} = -[\mathbf{U}^{-1}]_{(2,2)} \tag{16}$$

where $[\mathbf{U}^{-1}]_{(2,2)}$ denotes the element at lower right corner of the 2×2 matrix $\mathbf{U}^{-1}$. By substituting equations (14) and (15) into (16), in consequence, the derived CRB of ε can be represented as

$$\mathrm{CRB2} = \frac{3N^2QA_0\sigma_w^2}{2\pi^2\left[12Q^2(A_0C_0 - B_0^2) + N^2(Q^2-1)A_0^2\right]} \tag{17}$$

where $A_0 = \mathbf{s}_0^H\mathbf{s}_0$, $B_0 = \mathbf{s}_0^H\mathbf{D}_0\mathbf{s}_0$ and $C_0 = \mathbf{s}_0^H\mathbf{D}_0^2\mathbf{s}_0$. $\mathbf{D}_0$ is a $M \times M$ diagonal matrix whose (i,i)th element is equal to $i-1$ for $1 \le i \le M$. Unlike the expression of CRB1 in 10), where the result can be represented as a function of SNR, the derived CRB2 in Case II cannot be given in terms of SNR explicitly. By artificially restricting the square amplitude of frequency domain symbol to be a constant σ_s^2, we can obtain that $A_0 = M\sigma_s^2$. Therefore, the SNR may be written equivalently as

$$\mathrm{SNR} = \frac{\mathbf{s}_0^H\mathbf{s}_0}{M\sigma_w^2} \quad \text{or} \quad \mathrm{SNR} = \frac{\mathbf{s}^H\mathbf{s}}{N\sigma_w^2}. \tag{18}$$

Since the derived CRB2 has relation with $\mathbf{s}_0$ (through $\mathbf{A}_0, \mathbf{B}_0$ and $\mathbf{C}_0$), it means the performance that CRB2 can achieve depends on specific training symbol. Optimal training symbol for channel estimation can be found by computer search in [13]. However, the optimal training symbol for CFO estimation is still unknown and further investigation is required. In this paper, a Zadoff-Chu sequence is employed to generate the frequency domain training symbols [14].

Note that a similar situation in Case II has also been investigated in [10]. However, the derivation in [10] is not dedicated for OFDM systems, and thus there is not a particular equation that can be directly used for the comparison here. Therefore, we present a newly derived CRB2.

3.3 Discussion

As a comparison, the expression of CRB1 in (10) and that of CRB2 in (17) are plotted in Fig. 1. From Fig. 1, an obvious performance improvement can be observed by exploiting the exact training symbol, as well as the repetition property. This comparison can explicitly prove the conclusion stated above, i.e. by exploiting not only the repetition property but also the exact training symbol, more accurate CFO estimation can be obtained.

It is also noted that CRB1 can be improved by increasing Q. This is not surprising because the uncertainty of the training symbol decreases as Q increases. Therefore, we can get more information about the training symbol by adopting larger Q and the CRB1 is improved correspondingly. This observation indicates that larger Q should be adopted when only the repetition property is exploited. On the other side, we find that CRB2 is independent on Q. Since the exact training symbol is known, no more information about the training symbol can be acquired by increasing Q, and thus CRB2 keeps unchanged for different Q. Therefore, the selection of Q mainly depends on the implementation complexity when both repetition property and exact training symbol are exploited. As it will be shown in section 5.2, the complexity can increase in proportion to Q^2, and thus the minimal repetition patterns, that is $Q = 1$, is supposed to be the best choice.

4. Adaptive Numerical Method for ML-Estimation

4.1 Derivation of ML-Estimation

Recall the signal model in (3), the PDF of received vector $\mathbf{r}$ can be written as

$$f(\mathbf{r}; \mathbf{h}, \varepsilon) = \prod_{q=1}^{Q} f(\mathbf{r}_q; \mathbf{h}, \varepsilon). \tag{19}$$

In a frequency selective channel, the received $\mathbf{r}_q$ can be represented by

$$\mathbf{r}_q = \mathbf{F}_0 \mathbf{S}_0 \mathbf{h} e^{j\frac{2\pi\varepsilon}{Q}(q-1)} + \mathbf{w}_q. \tag{20}$$

Therefore, the PDF of $\mathbf{r}_q$ is given by

$$f(\mathbf{r}_q; \mathbf{h}, \varepsilon) = \frac{1}{(\pi\sigma_w^2)^L} \exp\left[-\frac{1}{\sigma_w^2} \left\| \mathbf{r}_q - \mathbf{F}_0 \mathbf{S}_0 \mathbf{h} e^{j\frac{2\pi\varepsilon}{Q}(q-1)} \right\|^2 \right]. \tag{21}$$

We can obtain the ML estimation of ε by maximizing the PDF in (19). As (19) can be further simplified by substituting (20) and (21) into (19), the estimation of ε may be obtained by equivalently maximizing the following $\Lambda_0(\mathbf{h}, \varepsilon)$

$$\Lambda_0(\mathbf{h}, \varepsilon) = -\left(\mathbf{r}^H \mathbf{r} - \mathbf{h}^H \mathbf{u} - \mathbf{u}^H \mathbf{h} + \mathbf{h}^H \mathbf{C} \mathbf{h} \right) \tag{22}$$

where

$$\mathbf{u} = \sum_{q=1}^{Q} \mathbf{S}_0^H \mathbf{F}_0^H \mathbf{r}_q \exp\left[-j\frac{2\pi\varepsilon}{Q}(q-1)\right], \tag{23}$$

$$\mathbf{C} = Q\mathbf{S}_0^H \mathbf{S}_0, \tag{24}$$

due to the following relation,

$$\max_{\{\mathbf{h}, \varepsilon\}} \Lambda_0(\mathbf{h}, \varepsilon) = \max_{\{\varepsilon\}} \left\{ \max_{\{\mathbf{h}\}} \Lambda_0(\mathbf{h}, \varepsilon) \right\}.$$

We can first derive the estimation of channel response $\mathbf{h}$. For a given ε, the Least Square (LS) estimation of $\mathbf{h}$ can be given by [12]

$$\hat{\mathbf{h}} = \mathbf{C}^{-1} \mathbf{u}. \tag{25}$$

By substituting this relation into (22), noting that $\mathbf{C}^H = \mathbf{C}$, we can obtain the ML estimation of ε as

$$\hat{\varepsilon} = \arg\max_{\{\varepsilon\}} \Lambda_1(\varepsilon) \tag{26}$$

where $\Lambda_1(\varepsilon) = \mathbf{u}^H \mathbf{C}^{-1} \mathbf{u}$.

To derive (26), the PDF in (21), where the training symbol (i.e. matrix $\mathbf{S}_0$) is considered to be known to the receiver, is employed, instead of a PDF where the training symbol is modeled as Gaussian noise (e.g. (9)). This guarantees that the proposed ML estimation algorithm exploits the exact training symbol, as well as the repetition property. It should be noted that a similar expression for CFO estimation can be found in [11]. This is not surprising because both algorithms employ the ML criterion, and thus lead to the same expression for CFO estimation. However, for the maximization of (26), a two-step search procedure is employed in [11].

The first step is carried out by comparing the cost function at a group of discrete CFO values. The second step is implemented by some interpolation method. However, the computational efficiency of this two-steps method is low due to exhaustive searching, so that it should be avoided in real time processing.

4.2 Proposed ANM Procedure

To solve (26) effectively, a new numerical procedure different from that adopted in [11] is described. In this procedure, we employ an Adaptive Numerical Method (ANM) to find the optimal ML estimation of ε. This ANM is based on the steepest descent scheme [16] and it can be carried out following three steps, as described in Tab. 1.

Step	Operation
1	Determine initial CFO ε_0, step size μ and threshold T
2	Calculate $\partial \mathbf{u}^H \mathbf{C}^{-1} \mathbf{u}/\partial\varepsilon$ using current ε_i, update $\varepsilon_{i+1} = \varepsilon_i + \mu \cdot \partial \mathbf{u}^H \mathbf{C}^{-1} \mathbf{u}/\partial\varepsilon$
3	if $\partial \mathbf{u}^H \mathbf{C}^{-1} \mathbf{u}/\partial\varepsilon < T$, stop; if $\partial \mathbf{u}^H \mathbf{C}^{-1} \mathbf{u}/\partial\varepsilon > T$, return to step 2.

Tab. 1. Adaptive Numerical Method.

Note that the obtained estimation of ε using ANM is the local maximum, so that the estimation range is determined by the initial value, as well as the pattern of $\Lambda_1(\varepsilon)$. Usually, we choose $\varepsilon_0 = 0$ as the initial value, so that the estimation range only depends on the pattern of $\Lambda_1(\varepsilon)$. The patterns of $\Lambda_1(\varepsilon)$ for $Q = 2, 4$ have been plotted in Fig. 2. As depicted in Fig. 2, the practical estimation ranges by using ANM for both $Q = 2, 4$ are $|\hat{\varepsilon}| < 1$. For ε that is out of the range $(-1, 1)$, ANM algorithm will converge to neighboring local maximum (e.g. $\varepsilon = 1.4$ in Fig. 2), and thus the estimator is not unbiased any more. The proposed algorithm is adaptive because it can automatically converge to the correct CFO value as long as the true CFO is inside the estimation range.
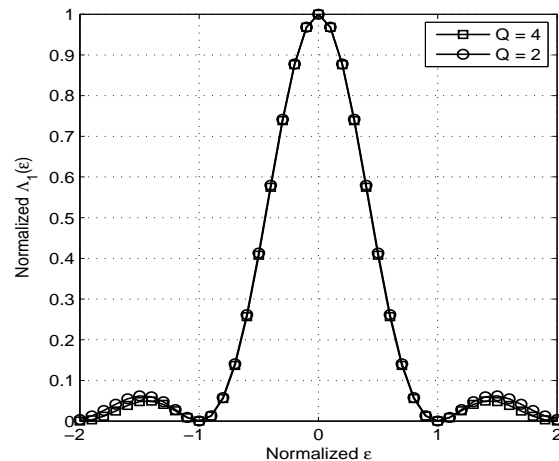
Fig. 2. Normalized $\Lambda_1(\varepsilon)$ for $Q = 2, 4$.

In a frequency selective channel, the received signal may experience severe fading, leading to very unstable received signal level. This changing received signal level can make the ANM algorithm unconverged and the proposed ML estimation may also malfunction. To mitigate variation of received signal level, we employ normalized $\partial\Lambda_1(\varepsilon)/\partial\varepsilon$, instead of directly using of $\partial\Lambda_1(\varepsilon)/\partial\varepsilon$, to perform step 3 in Tab. 1, i.e.

$$\frac{1}{\mathbf{r}^H\mathbf{r}}\left[\frac{\partial\Lambda_1(\varepsilon)}{\partial\varepsilon}\right] \gtrless T. \tag{27}$$

5. Performance Analysis

5.1 Mean and Variance

In this section, we present some analysis on the mean and variance performance on the proposed algorithm.

The mean of proposed ML estimator can be assessed using the method indicated in [15]. Assuming the SNR is high enough, the mean of proposed ML estimator can be approximated by

$$E(\hat{\varepsilon}) \approx \varepsilon - \frac{E\left[\partial\Lambda_1(\varepsilon)/\partial\varepsilon\right]}{E\left[\partial^2\Lambda_1(\varepsilon)/\partial\varepsilon^2\right]}. \tag{28}$$

For the integrity of the formal presentation of this paper, detailed derivation of the right hand side of equation above is found in Appendix, we only present the result here. As indicated in Appendix, it is found that

$$E(\hat{\varepsilon}) = \varepsilon. \tag{29}$$

This relation means that the proposed ML estimator is unbiased, even in frequency selective channel. To avoid the cumbersome derivation of variance performance, we use CRB2 obtained in Section 3 to approximate the variance expression of proposed estimator, since the variance of ML estimation can achieve the lower bound determined by CRB at high SNR [12]. It will be seen in next section that this approximation is appropriate. Under that approximation, the variance of the proposed estimator can be given by

$$\text{var}(\hat{\varepsilon}) = \frac{3N^2QA_0\sigma_w^2}{2\pi^2\left[12Q^2(A_0C_0 - B_0^2) + N^2(Q^2-1)A_0^2\right]}. \tag{30}$$

5.2 Computation Complexity

The computation complexity is investigated in this section in terms of complex additions (cas) and complex multiplies (cms). Since the proposed algorithm is an iterative method, we only calculated the cas and cms required in each iteration. During each iteration, we should calculate the term $\partial\mathbf{u}^H\mathbf{C}^{-1}\mathbf{u}/\partial\varepsilon$. As shown in (23) and (24), $\mathbf{S}_0^H\mathbf{S}_0$ and $\mathbf{S}_0^H\mathbf{F}_0^H$ are fixed, so they can be precomputed and thus no complexity is caused. Therefore, we need $Q^2N^2 - 1$ cas and $Q^2(N^2 + N + 1)$ cms in total.

6. Numerical Results

Some numerical results are given in this section to verify the theoretical analysis and extend the analytical analysis. An OFDM system with $N = 64$ subcarriers is employed in this simulation. We use Zadoff-Chu sequence to generate the frequency domain training symbols. The length and root value of employed Zadoff-Chu sequence are N/Q and 18, where $Q = 2, 4$. The generated Zadoff-Chu sequence symbols are equally spaced by $Q - 1$ zeros. To ensure that the comparison between the case of AWGN channel and that of FSRF channel is believable, the power of each path in FSRF channel should coincide with the following relation $\sum_{l=1}^{6}\sigma_l^2 = 1$. For simplicity, the unitary power are equally allocated to all those 6 paths. As a comparison, the methods in [7] and [8], which exploit the repetitions only for CFO estimation, are also investigated in the simulation. In the simulation, the initial parameters of ANM algorithm are given in the following

$$\varepsilon_0 = 0, \mu = 0.001, T = 0.01.$$

Fig. 3 illustrates the average estimation result versus the real CFO value with proposed ML estimator in this paper. This figure is plotted under the condition that SNR = 10 dB. It should be noted that Fig. 3 shows both the case of AWGN channel and the case of FSRF channel. In both cases, the proposed estimator is unbiased within given estimation range, which coincides with the conclusion we have derived in Section IV. Fig. 3 also shows that the estimation range is as large as $|\hat{\varepsilon}| < 1$ for both $Q = 2$ and $Q = 4$, which is also a derived result above. For CFO value that is out of the estimation range, the ANM algorithm converges to neighboring local maximum (cf. Fig. 2), thus the estimator is not unbiased any more.

Fig. 4 shows the MSE performance of proposed ML estimator, as well as the conventional methods, for $Q = 2$ in AWGN channel. From Fig. 4, it can be seen that the performance of those three estimators can almost coincide with corresponding CRBs. Due to the performance improvement of CRBs, the proposed ML estimator may also outperform conventional methods. As depicted in Fig. 4, the performance improvement at small SNR can be as large as 2 dB. It should also be noted that conventional methods proposed in [7] and [8] have the same performance for $Q = 2$. This is because there are only two repetition patterns that can be used, thus those two estimators work in the same manner.

Fig. 5 gives the MSE versus SNR curves for $Q = 4$ in AWGN channel. As depicted in Fig. 5, the proposed ML estimator still outperforms the conventional methods, however, the quantity of performance improvement descends. At small SNR, about 1 dB SNR can be saved by using the proposed ML estimator rather than conventional methods. This can be accounted for as follows: due to increased Q, the number of repetition patterns increases in the training symbol, thus the performance of conventional methods those exploit only repetition property also improves accordingly. It

is also noted that the conventional method proposed in [8] gives better performance than the one proposed in [7]. This is because the repetition property has been fully exploited using the conventional method proposed in [8]. From Fig. 5, it can be seen that the method in [8] has already achieved the CRB1 bound. It means we cannot find an algorithm that outperforms the method proposed in [8] by only exploiting the repetition property of the training symbol. To further improve the performance, the exact training symbol should also be utilized. As depicted in Fig. 5, the proposed ML estimator in this paper can outperform those conventional methods, due to not only exploiting the repetition property but also the exact training symbol.

The performance of those three estimators in FSRF channel with $Q = 2$ are shown in Fig. 6. As expected, both conventional methods proposed in [7] and [8] still have the same performance even in frequency selective channel. A significant performance improvement can be observed in Fig. 6 by using the proposed ML estimator in this paper rather than those conventional algorithms. At small SNR, the SNR saving can be as large as 3 dB. The CRB1 and CRB2 in AWGN channel are also plotted in Fig. 6 in order to make a comparison with the performance in FSRF channel. As it can be seen in Fig. 6, due to channel fading, the performance in FSRF channel performs significantly worse than that in AWGN channel.

Fig. 7 plots the performance curves in FSRF channel for $Q = 4$. As there are more than two repetition patterns can be utilized, the estimator proposed in [8] outperforms the estimator proposed in [7], due to full exploitation of the repetition property. The proposed ML estimator in this paper shows the optimal performance in these three estimator, because of the utilization of the exact training symbol. By using the proposed ML estimator rather than conventional methods, 2 dB and 4 dB SNR can be saved respectively in FSRF channel for $Q = 4$.

To evaluate the convergence performance of the proposed algorithm, we carried out a simulation in the AWGN channel with SNR = 25 dB and $Q = 4$. Different step sizes are considered in the simulation, and the simulation results are shown in Fig. 8. As shown, the proposed algorithm can converge for both step sizes. It may converge fast when μ is large. This is because the increment in each iteration is large due to adoption of large step size. However, the cost is the poor asymptotical performance. Large step may cause inaccurate estimation when estimate is close to the true CFO. On the contrary, small step size can lead to more accurate asymptotical performance, at the cost of slower convergence rate.

7. Conclusion

Through the comparison of corresponding CRBs, it is shown that the CFO estimation performance can be improved by exploiting the repetition property and the exact training symbol. The selection of Q for different situations

is also discussed in this paper. For exploiting the repetition property and the exact training symbol, a ML-estimation has been derived in this paper. To save computational complexity for solving the likelihood function, a new numerical procedure is proposed in this paper. Numerical results are also presented to demonstrate the conclusions in this paper.
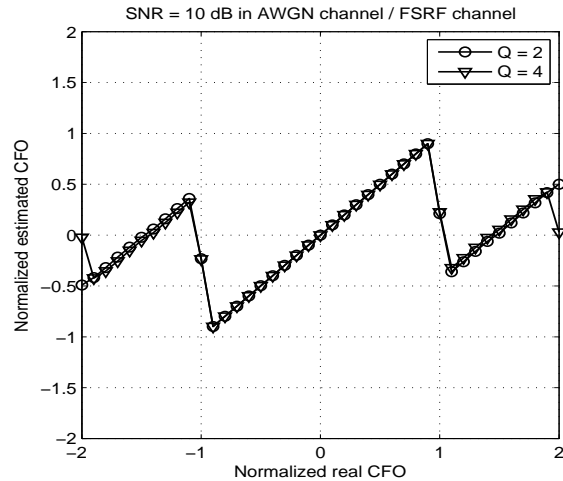
Fig. 3. Estimation range in AWGN channel for $Q = 2, 4$.
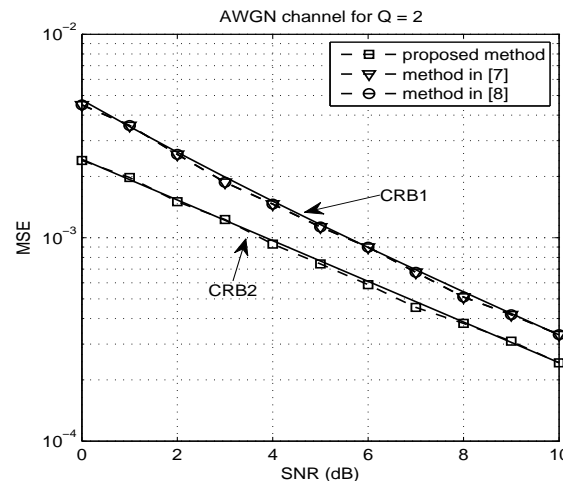
Fig. 4. Estimation performance in AWGN channel for $Q = 2$.
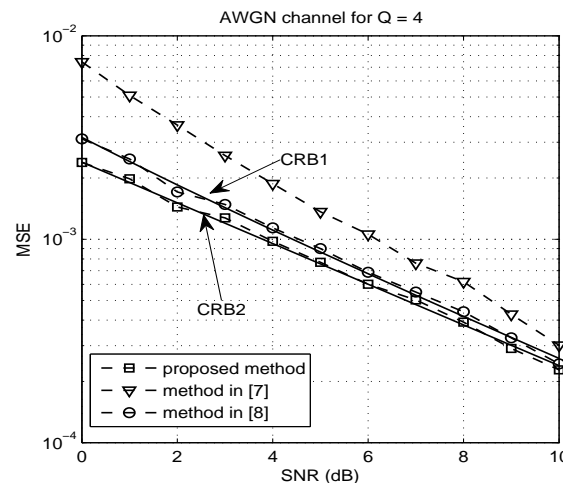
Fig. 5. Estimation performance in AWGN channel for $Q = 4$.
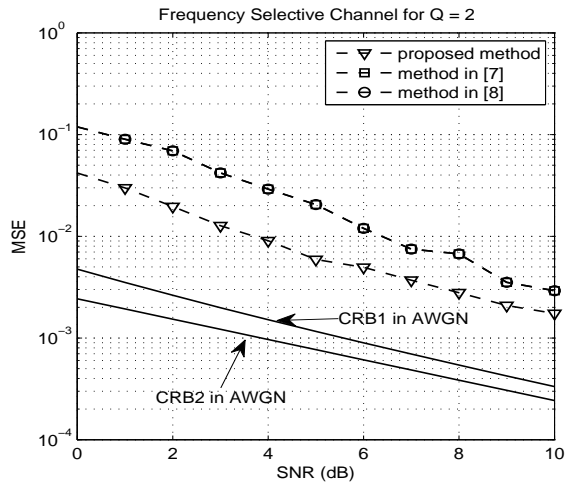
Fig. 6. Estimation performance in frequency selective channel for $Q = 2$.
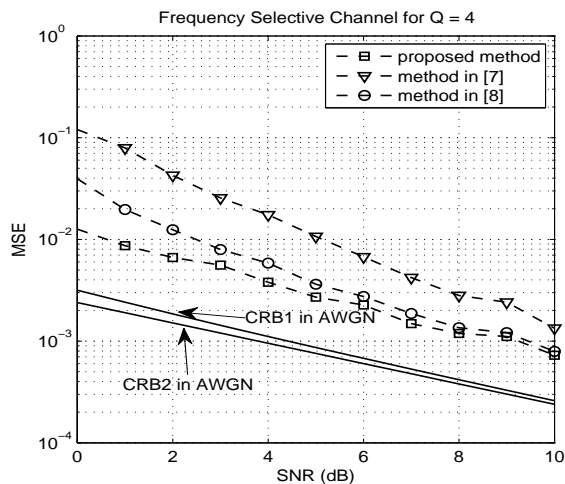
Fig. 7. Estimation performance in frequency selective channel for $Q = 4$.
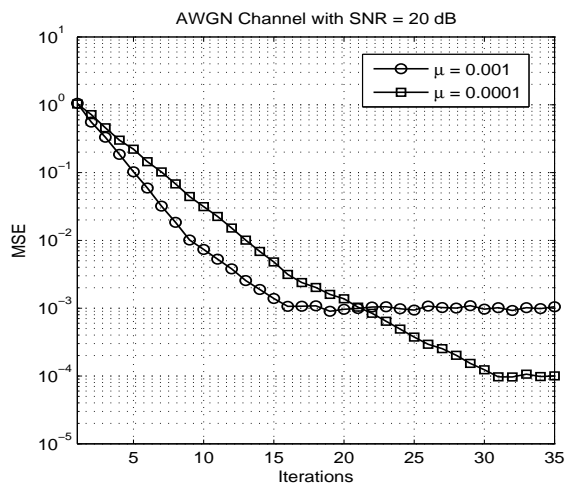
Fig. 8. Convergence performance in AWGN channel with SNR = 20 dB for $Q = 4$.

Acknowledgements

References

[1] BINGHAM, J. A. C. Multicarrier modulation for data transmission: An idea whose time has come. *IEEE Communications Magazine*, 1990, vol. 28, no. 5, p. 5-14.

[2] MAY, T., ROHLING, H., ENGELS, V. Performance analysis of Viterbi decoding for 64-DAPSK and 64-QAM modulated signal. *IEEE Transactions on Communication*, 1998, vol. 46, no. 2, p. 182 - 190.

[3] REIMERS, U. Digital video broadcasting. *IEEE Communications Magazine*, 1998, vol. 36, no. 6, p. 104 - 110.

[4] *Local and Metropolitan Area Networks-Part 16, Air Interface for Fixed Broadband Wireless Access Systems*. IEEE Standard IEEE 802.16e.

[5] SCHMIDL, T. M., COX, D. C. Robust frequency and timing synchronization for OFDM. *IEEE Transactions on Communications*, 1997, vol. 45, no. 12, p. 1613 - 1621.

[6] MORELLI, M., MENGALI, U. An improved frequency offset estimator for OFDM applications. *IEEE Communications Letters*, 1999, vol. 3, no. 3, p. 75 - 77.

[7] MINN, H., BHARGAVA, V. K., LETAIEF, K. B. A robust timing and frequency synchronization for OFDM systems. *IEEE Transactions on Wireless Communications*, 2003, vol. 2, no. 4, p. 822 - 839.

[8] CHOI, J. W., LEE, J. Joint ML estimation of frame timing and carrier frequency offset for OFDM systems employing time-domain repeated preamble. *IEEE Transactions on Wireless Communications*, 2010, vol. 9, no. 1, p. 311 - 317.

[9] CHENG, M., CHOU, C. Maximum-likelihood estimation of frequency and time offsets in OFDM systems with multiple sets of identical data. *IEEE Transactions on Signal Processing*, 2006, vol. 54, no. 7, p. 2848 - 2852.

[10] MINN, H., FU, X., BHARGAVA, V. K. Optimal periodic training signal for frequency offset estimation in frequency-selective fading channels. *IEEE Transactions on Communications*, 2006, vol. 54, no. 6, p. 1081 - 1096.

[11] MORELLI, M., MENGALI, U. Carrier-frequency estimation for transmissions over selective channels. *IEEE Transactions on Communications*, 2000, vol. 48, no. 9, p. 1580 - 1589.

[12] KAY, S. M. *Fundamentals of Statistical Signal Processing: Estimation Theory*. Englewood Cliffs (NJ, USA): Prentice Hall, 1993.

[13] TELLAMBURA, C., PARKER, M. G., GUO, Y. J., SHEPHERD, S. J., BARTON, S. K. Optimal sequencws for channel estimation using discrete Fourier transform techniques. *IEEE Transactions on Communications*, 1999, vol. 47, no. 2, p. 230 - 238.

[14] MOW, W. H., LI, S. Y. R. Aperiodic autocorrelation properties of perfect polyphase sequences. In *Singapore ICCS/ISITA '92*. Singapore, 1992, p. 1232 - 1234.

[15] MEYRS, M. H., FRANKS, L. E. Joint carrier phase and symbol timing recovery for PAM systems. *IEEE Transactions on Communications*, 1980, vol. 28, no. 8, p.1121 - 1129.

[16] HAYKIN, S. *Adaptive Filter Theory. Fourth Edition*. Upper Saddle River (NJ, USA): Prentice Hall, 2001.

Appendix: Derivation of (28)

In this appendix, we derive the relations of right hand side of (28). By substituting (23) and (24) into (26), $\Lambda_1(\varepsilon)$ may be rewritten as

$$\Lambda_1(\varepsilon) = \frac{1}{Q} \sum_{m=1}^{Q} \sum_{n=1}^{Q} \mathbf{r}_m^H \mathbf{F}_0 \mathbf{P} \mathbf{F}_0^H \mathbf{r}_n \exp\left[j\frac{2\pi\varepsilon}{Q}(m-n) \right] \quad (31)$$

where $\mathbf{P} = \mathbf{S}_0 \left(\mathbf{S}_0^H \mathbf{S}_0 \right)^{-1} \mathbf{S}_0^H$ is the projection matrix. Noting the following relations,

$$\partial \mathbf{F}_0 / \partial \varepsilon = j\frac{2\pi}{N} \mathbf{D}_0 \mathbf{F}_0, \quad (32)$$

$$\partial \mathbf{F}_0^H / \partial \varepsilon = -j\frac{2\pi}{N} \mathbf{D}_0 \mathbf{F}_0^H, \quad (33)$$

here, $\mathbf{D}_0$ is a $M \times M$ diagonal matrix whose (i,i)th element is equal to $i-1$ for $1 \le i \le M$, then the first order differentiation of $\Lambda_1(\varepsilon)$ can be represented as

$$\frac{\partial \Lambda_1(\varepsilon)}{\partial \varepsilon} = j\frac{2\pi}{QN} \sum_{m=1}^{Q} \sum_{n=1}^{Q} \mathbf{r}_m^H \mathbf{F}_0 \mathbf{B}^{(m,n)} \mathbf{F}_0^H \mathbf{r}_n e^{j\frac{2\pi\varepsilon}{Q}(m-n)} \quad (34)$$

where $\mathbf{B}^{(m,n)} = \mathbf{D}_0 \mathbf{P} - \mathbf{P} \mathbf{D}_0 + (m-n) M \mathbf{P}$. Substituting (20) into (34), the resulting differentiation of $\Lambda_1(\varepsilon)$ may be rewritten as

$$\frac{\partial \Lambda_1(\varepsilon)}{\partial \varepsilon} = j\frac{2\pi}{QN} \sum_{m=1}^{Q} \sum_{n=1}^{Q} \Gamma_{(m,n)} \quad (35)$$

where

$$\begin{aligned}
\Gamma_{(m,n)} = & \ \mathbf{h}^H \mathbf{S}_0^H \mathbf{B}^{(m,n)} \mathbf{S}_0 \mathbf{h} + \\
& \ \mathbf{h}^H \mathbf{S}_0^H \mathbf{B}^{(m,n)} \mathbf{F}_0^H \mathbf{w}_n e^{-j\frac{2\pi\varepsilon}{Q}(n-1)} + \\
& \ \mathbf{w}_m^H \mathbf{F}_0 \mathbf{B}^{(m,n)} \mathbf{S}_0 \mathbf{h} e^{j\frac{2\pi\varepsilon}{Q}(m-1)} + \\
& \ \mathbf{w}_m^H \mathbf{F}_0 \mathbf{B}^{(m,n)} \mathbf{F}_0^H \mathbf{w}_n.
\end{aligned} \quad (36)$$

Since $\mathbf{P}$ is the projection matrix, it can be obtained that

$$\mathbf{h}^H \mathbf{S}_0^H \mathbf{D}_0 \mathbf{P} \mathbf{S}_0 \mathbf{h} = \mathbf{h}^H \mathbf{S}_0^H \mathbf{P} \mathbf{D}_0 \mathbf{S}_0 \mathbf{h}. \quad (37)$$

Bearing in mind the relation in (37), we then derive that

$$\begin{aligned}
\Gamma_{(m,n)} = & \ M(m-n) \mathbf{h}^H \mathbf{S}_0^H \mathbf{P} \mathbf{S}_0 \mathbf{h} + \\
& \ \mathbf{h}^H \mathbf{S}_0^H \mathbf{B}^{(m,n)} \mathbf{F}_0^H \mathbf{w}_n e^{-j\frac{2\pi\varepsilon}{Q}(n-1)} + \\
& \ \mathbf{w}_m^H \mathbf{F}_0 \mathbf{B}^{(m,n)} \mathbf{S}_0 \mathbf{h} e^{j\frac{2\pi\varepsilon}{Q}(m-1)} + \\
& \ \mathbf{w}_m^H \mathbf{F}_0 \mathbf{B}^{(m,n)} \mathbf{F}_0^H \mathbf{w}_n.
\end{aligned} \quad (38)$$

Due to the following relations,

$$M\left[\sum_{m=1}^{Q} \sum_{n=1}^{Q} (m-n) \right] \mathbf{h}^H \mathbf{S}_0^H \mathbf{P} \mathbf{S}_0 \mathbf{h} = 0, \quad (39)$$

$$E\left[\mathbf{h}^H \mathbf{S}_0^H \mathbf{B}^{(m,n)} \mathbf{F}_0^H \mathbf{w}_n e^{-j\frac{2\pi\varepsilon}{Q}(n-1)} \right] = 0, \quad (40)$$

$$E\left[\mathbf{w}_m^H \mathbf{F}_0 \mathbf{B}^{(m,n)} \mathbf{S}_0 \mathbf{h} e^{j\frac{2\pi\varepsilon}{Q}(m-1)} \right] = 0, \quad (41)$$

the mean of (35) can be simplified as

$$E\left[\frac{\partial \Lambda_1(\varepsilon)}{\partial \varepsilon} \right] = j\frac{2\pi}{QN} \sum_{m=1}^{Q} \sum_{n=1}^{Q} \mathbf{z}_m^H \mathbf{B}^{(m,n)} \mathbf{z}_n \quad (42)$$

where $\mathbf{z}_i = \mathbf{F}_0^H \mathbf{w}_i$ for $i = 1, 2, \cdots, Q$ and thus $E\left(\mathbf{z}\mathbf{z}^H \right) = \sigma_w^2 \mathbf{I}$. As $\mathbf{z}_i$ is white noise, (39) can rewritten as

$$E\left[\frac{\partial \Lambda_1(\varepsilon)}{\partial \varepsilon} \right] = j\frac{2\pi}{QN} \sum_{m=1}^{Q} \sum_{i=1}^{M} \sigma_w^2 \mathbf{B}_{(i,i)}^{(m,m)} \quad (43)$$

where $\mathbf{B}_{(i,i)}^{(m,m)}$ indicates the (i,i)th element in matrix $\mathbf{B}^{(m,m)}$. After some algebra, it is found that all the diagonal elements of matrix $\mathbf{B}_{(i,i)}^{(m,m)}$ ($1 \le m \le Q, 1 \le i \le M$) are equal to zeros. Therefore, it is finally concluded that

$$E\left[\frac{\partial \Lambda_1(\varepsilon)}{\partial \varepsilon} \right] = 0. \quad (44)$$

In consequence, the relation in (29) is obtained.

About Authors...

Yinsheng LIU received the B.S. degree from North China Electric Power University, Baoding, China, and the M.S. degree from Beijing Jiaotong University, Beijing, China, in 2007 and 2009, respectively, all in communication and information system. He is currently pursuing his Ph.D degree at Beijing Jiaotong University, Beijing, China. His research interests include wireless communication system and digital signal processing.

Zhenhui TAN Professor and Ph.D. in Communications and Information Systems, was born on Feb. 18, 1944 in Yangzhou, Jiangsu Province. He graduated from Beijing Jiaotong University (BJTU) and majored in wireless communications in 1967. He received his master's degree in 1981 at BJTU and Ph.D. in 1987 at Southeast University, respectively. From 1998 to 2008, Professor Tan was the President of BJTU. From 1995 to 1998, Professor Tan was the Vice President of BJTU. From 1993 to 1995, Professor Tan was the Director of Department of Communications and Signal Control Engineering in BJTU. From 1990 to 1993, Tan studied as visiting scholar at Mons Technology College, Belgium and at University of Waterloo, Canada. Professor Tan is a member of the National Hi-Tech Project's Specialist Committee for three consecutive tenures, a member of the Evaluation Committee for Academic Degree Affairs of the State Council for two consecutive tenures, a member of Specialist Committee for Postdoctoral Degree Affairs, director of electrical information science and engineering teaching guidance committee of Ministry of Education, a member of Supervision Committee of Natural Science Foundation of China (NSFC). Professor Tan is also a Fellow of China Institute of Communications (CIC), Vice director of Academic Committee of CIC. A Fellow of China Institute of Railway (CIR), Vice director of Committee for Control Engineering of CIR, a member of the editorial boards of both Chinese Journal of Electronics and Journal of the China Railways.